The American Society of Mechanical Engineers

Reprinted From
DE-Vol. 55, Reliability, Stress Analysis, and Failure Prevention
Editor: Richard J. Schaller
Book No. G00816 - 1993

A DEFORMATION AND LIFE PREDICTION OF A CIRCUMFERENTIALLY REINFORCED SIC/TI 15-3 RING

S. M. Arnold
NASA Lewis Research Center
Cleveland, Ohio

T. E. Wilt
University of Toledo
Toledo, Ohio

ABSTRACT

A computational methodology has been developed to predict the fatigue life of typical aerospace components, here the specific example is a circumferentially reinforced SiC/Ti-15-3 compressor ring designed for applications at 800° F. The analysis encompasses both a static burst pressure prediction and a life assessment of the cladded ring. A three dimensional stress analysis was performed using MARC, a nonlinear finite element code, wherein both the matrix cladding and the composite core were assumed to behave elastic-plastic. The composite core behaviour was represented using Hill's anisotropic continuum based plasticity model with bilinear hardening. Similarily, the matrix cladding was represented by an isotropic perfectly plastic model. The load-displacement (i.e., internal pressure versus radial deflection) response of the ring was used to determine the static burst pressure.

The life assessment was conducted using the stress analysis results, in conjunction with a recently developed multiaxial, isothermal, continuum damage mechanics model for the fatigue of unidirectional metal matrix composites. This model is phenomenological, stress based, and assumes a single scalar internal damage variable, the evolution of which is anisotropic. The accumulation of damage is included in the stress analysis by employing the concept of effective stress. In the current application, however, the damage model is computationally-decoupled from the finite element solution. The spocific methodology for this computationally-decoupled fatigue damage simulation is outlined and results are given in terms of the evolution of damage and design life curves.

INTRODUCTION

Advanced compressor rotor designs, incorporating titanium metal matrix composite (TMC) rings embedded within an integrally bladed rotor (IBR), are projected to have significant benefits compared to the baseline nickel and titanium rotors currently in service, including decreased weight and increased rotor speeds. However, for advanced compression systems to realize the full potential benefits offered by TMC's, design and life prediction systems and fabrication techniques for TMC ring inserts must be developed and demonstrated. To this end, NASA and Pratt & Whitney (P&W) Aircraft Division entered into a cooperative research program with the goal of developing and experimentally verifying fatigue life prediction models for metal matrix composites, and in particular, TMC's. Emphasis was placed on ultimately modeling the static burst and cyclic fatigue lives of sub-scale TMC rings which were respresentitive of those used in advanced compressor rotor designs. The selected material system was SCS-6/Ti-15V-3Cr-3Sn-3Al. The SCS-6 fiber is a 142 micron diameter, chemically vapor deposited, SiC fiber with a double carbon coating for improved chemical compatibility with titanium matrices. Although, Ti 15-3, is not of primary interest for gas turbine engine applications (due to upper use temperature capability, oxidation resistance, and burn resistance limitations) it was selected as the matrix system for this program because of established processing parameters, demonstrated reproducibility of mechanical properties and near-term availability in the form required for panel and ring processing.

The objective of the present study is to perform an analysis encompassing both a static burst pressure prediction and life assessment of a circumferentially reinforced SiC/Ti-15-3 cladded ring designed for application at 800° F. A major concern in developing an MMC deformation and life prediction methodology is the question of scale-up associated with characterizing a given theory with test results from relatively thin MMC panels (test coupons) and than applying this theory to relatively large volume MMC structures. As a result, to verify the analysis methodology for actual engine component designs, the test conditions for the sub-scale rings were chosen to simulate typical gas turbine engine fan or compressor operating conditions.

The stress analysis is conducted using MARC, a nonlinear finite

element code, wherein both the matrix cladding and composite core are assumed to behave elastic-plastic. The life assessment is conducted using the stress analysis results, in conjunction with a recently developed multiaxial, isothermal, continuum damage mechanics model for the fatigue of unidirectional metal matrix composites. This model is phenomenological, stress based, and assumes a single *scalar* internal damage variable, the evolution of which is anisotropic. A unique aspect of this life model is the ability to include the accumulation of damage into the stress analysis by employing the concept of effective stress. In this way the redistribution of stresses, on the structural level, due to damage initiation and propagation can be accounted for conveniently and consistently. In the current application, the damage model is computationally-decoupled from the finite element solution, in that, the life assessment calculations are performed by "post-processing" the finite element deformation analysis results separately. Each deformation analysis and subsequent post life assessments represent various increments (or stages) of the total life. The specific methodology for this computationally-decoupled fatigue damage simulation is outlined and results are given in terms of the evolution of damage and design life curves.

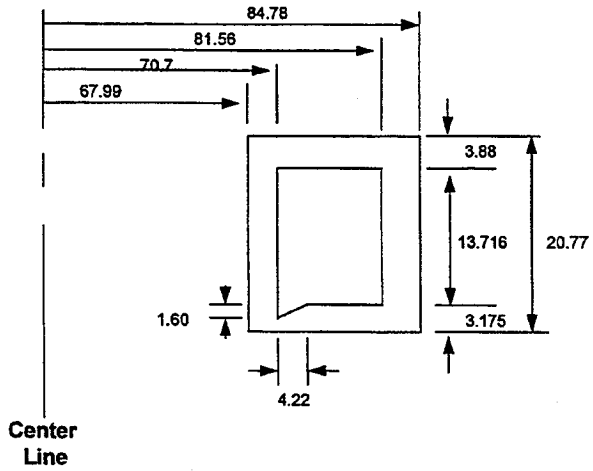

FIGURE 1: GEOMETRY OF AS-FABRICATED MMC RING

DEFORMATION ANALYSIS

The actual ring was idealizedaccording to the results of the NDE analysis (Baaklini et al. (1993)) and information regarding the actual testing of the rings. Pratt & Whitney's hydraulic actuator burst rig was used to perform both the static burst test and the low cycle tension tension fatigue tests. The test rig consisted of 24 hydraulic actuators positioned around a high temperature test chamber that are capable of applying over one million pounds of uniform load against the inner diameter of the composite ring at temperatures exceeding 1500°F. The tests were performed under load control using a System 4000 data acquisition system. The actual cross section of ring one, obtained from the average of 35 CT scans is shown in Fig. 1. All three SiC/Ti 15-3 rings contained 57 plies with approximately 33 volume percent of fibers.

A deformation analysis was performed on the idealized composite ring in order to determine the load versus displacement response and thus static burst pressure. A three dimensional finite element model of one quarter of the ring, which consists of a composite core surrounded by matrix cladding, was constructed, see Fig 2. The finite element model consisted of 1701 nodes and 1280 8-noded 3-D elements (MARC element number 7). A uniform pressure load was applied to all of the elements that form the inner diameter face of the ring. The boundary conditions were as follows: $w = 0$ for all nodes at z=0, and symmetry conditions at each end of the quarter ring, i.e., $v = 0$ for all nodes at y=0, $u = 0$ for all nodes at x=0. In this analysis a number of simplifying assumptions were made with respect to residual stresses, ring geometry, and the material characterization.

The assumptions with respect to residual stresses are as follows. All residual stresses generated during the fabrication cycle are assumed to be eliminated during the heat treatment process. Consequently, only those residual stresses due to cool down from 1292°F to room temp and heat-up to the application temp of 800°F are calculated. Macro residual stresses are accounted for by considering the CTE mismatch between matrix cladding and the composite core. Whereas, micro residual stresses (i.e., the CTE mismatch between fiber and matrix) are accounted for in the uniaxial tensile specimen data and consequently are assumed to be included in the coefficients of the constitutive model.

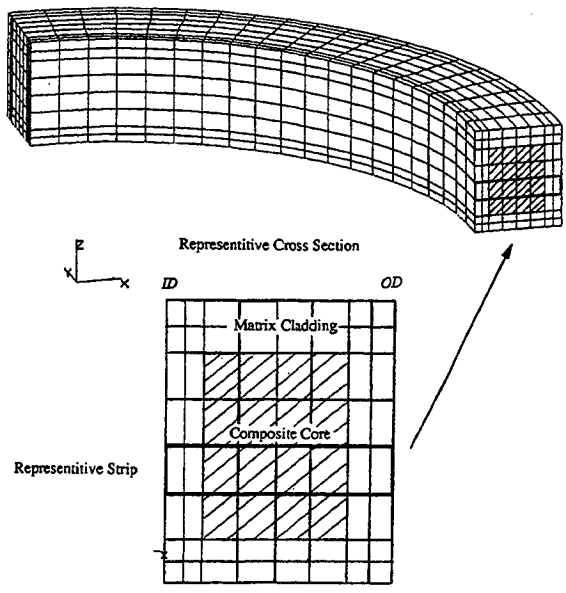

FIGURE 2: FINITE ELEMENT MODEL OF MMC RING

The assumptions with respect to ring geometry are as follows. The assumption of perfect bonding between composite core and matrix cladding was made. The ring was assumed to be defect free, in that initial damage due to fabrication was not included in either the deformation or life analyses. Initial damage can easily be included once a relationship between density changes (CT measurements) and mechanical properties is established. The offset of the inner core was accounted for in the finite element analysis, but not the presence of the cusp. The ring, as well as load application, was assumed to be circular and axisymmetric. Finally, the fiber spacing was assumed to be periodic and any deviation was assumed to be included in the tensile data.

Lastly, the assumptions with respect to material characterization are as follows. The matrix cladding was assumed to behave elastic/perfectly plastic. The composite core was assumed to exhibit either perfectly plastic or bilinear hardening behavior. The mechanical composite properties were taken to be temperature independent, because of limited data characterizing the temperature dependence, whereas the temperature dependence of the coefficient of thermal expansion (CTE) was incorporated.

CONSTITUTIVE MODEL

The composite core was idealized as a pseudo-homogeneous transversely isotropic material that is described by an anisotropic elastic-plastic constitutive model (Robinson and Pastor (1992), Hill (1983)). The matrix cladding is taken to be isotropic and elastic perfectly-plastic. A recent transversely isotropic perfectly-plastic constitutive model, put forth by (Robinson and Pastor (1992)) was used to characterize the matrix and composite core. The associated material parameters are shown in Table 1. The material parameters were obtained from data generated during the P&W/NASA LeRC cooperative program (Gravett (1990)). Note that this model is also equivalent to the more general (in that hardening and other forms of anisotropy can be included) Hill's anisotropic model (Hill (1983)). Henceforth, whenever bilinear hardening is referred to, the model used is that of Hill's with the associated material parameters given in Table 1. Figures 3 and 4 illustrate the excellent correlation between experiment (Lerch (1991)) and theory of the longitudinal (0°) and transverse (90°) tensile response when using an isothermal, transversely isotropic, plasticity model. The two cases considered here are perfect plasticity (wherein $H = 0$, see Fig. 3) and the bilinear hardening case wherein $H \neq 0$, see Fig. 4. Note, that for the perfectly plastic correlation a secant like elastic longitudinal modulus of 184 Gpa resulted from the assumption that the longitudinal response was purely elastic up to failure (i.e., $e_f = 0.0078$ and $\sigma_{ultimate} = 1436$ MPa). On the other hand, in the bilinear case all material constants were obtained by fitting the longitudinal tensile response, thus explaining the difference in the composite longitudinal elastic moduli in Table 1.

DEFORMATION RESULTS

To gain confidence in the finite element analysis and to assess

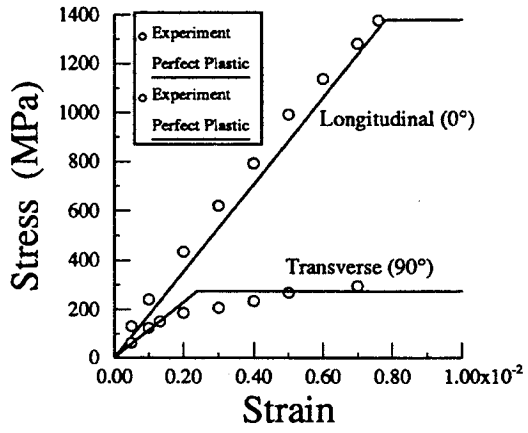

FIGURE 3: PERFECT PLASTICITY MODEL CORRELATION WITH EXPERIMENTAL DATA

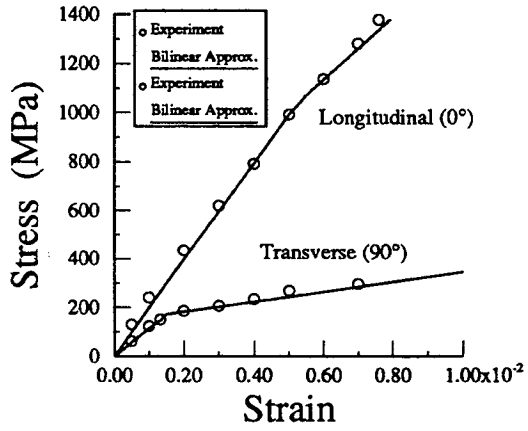

FIGURE 4: BILINEAR HARDENING MODEL CORRELATION WITH EXPERIMENTAL DATA

the impact of the assumed constitutive behavior and residual stress state, various comparison calculations were made. First, analytical limit loads were calculated, using the upper and lower bound expressions given by Robinson (Robinson and Pastor (1992)), for the cases of a solid composite and solid matrix ring. Clearly, in these cases no CTE mismatch between matrix cladding and composite core, and thus no residual stress, is present. The results are shown in Table 2. Next, a comparison between analytical first yielding and that calculated using the finite element method was made. Agreement was very good.

Figure 5, shows the internal pressure versus radial displacement of the actual cladded ring (see Fig. 1) and illustrates the impact of assuming an elastic-plastic versus elastic constitutive behavior response, as well as the effect of including, or excluding, the structural residual stress developed during consolidation. Clearly, the final limit load is unaffected by the residual stress; however, first

yielding is significantly affected. Also, it is apparent that inclusion of plasticity has a greater impact on the resulting limit load than does residual stress. That is, a burst pressure calculated using an elastic analysis with an appropriate strain to failure criteria far

Table 1: MATERIAL PARAMETERS

Matrix Properties (MPa, C)

Temp	E	ν	α (10^{-6})	σ_y
21.	88.	0.32	2.5	710.
300..	81.	0.32	2.872	582.
530.	74.	0.32	3.09	450.
700.	68.	0.32	3.24	207.

Composite Properties - SiC/Ti 15-3 (35% fvr)
Perfect Plasticity (MPa)

E_L	E_T	ν_L	ν_T	σ_y	H	ω
184.	114.	0.28	0.32	276.	0	5.0

Bilinear Hardening (MPa)

E_L	E_T	ν_L	ν_T	σ_y	H	ω
198.	114.	0.28	0.32	179.	19306.	5.54

Coefficient of Thermal Expansion (C)

Temp.	α_L (10^{-6})	α_T (10^{-6})
21.1	1.6	1.47
100.	1.66	2.36
200.	1.75	3.110
300.	1.82	3.110
700.	1.82	3.110

exceeds that calculated using an elastic-plastic analysis and as one might expect, the influence of residual stresses on the elastic stress analysis results far exceeds that of an elastic-plastic.

Figure 6, shows a plot of pressure versus circumferential strain for the cases of a perfectly plastic and bilinear hardening material. In both cases, residual stresses have been included in the analysis. For the assumption of perfect plasticity the limit load (burst pressure) is approximately 207 MPa at a circumferential strain of 0.8%. The strain to failure criteria is based on the failure strain of uniaxial test coupons, which occur at approximately 0.78%. Applying a similar strain to failure criteria to the bilinear hardening response curve, at the inner diameter, results in a burst pressure of approximately 214 MPa. If we consider the outer diameter response, see Fig. 7, the burst pressure is 227 MPa. The closeness of the inner and outer burst pressures gives one confidence in the rapid failure of the entire ring, thus suggesting an average of the two limits, i.e., P_L = 221 MPa.

Prior to P&W conducting the actual static burst test on the MMC ring, a prediction (based on the bilinear hardening response) of the deformation response and ultimate burst pressure was thought to be the most realistic. This statement was verified by comparing the experimentally obtained pressure versus radial deflection response at the outer diameter (OD), for rings one and

Table 2: COMPARISON OF LIMIT LOADS

	Analytical Plane Strain	F.E.	Analytical Plane Stress
Solid Core	305.	269.	256.
Solid Matrix	130.	119.	118.
Cladded Ring	--	207.	--

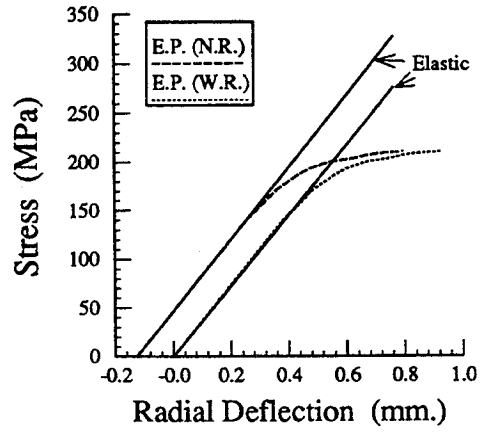

FIGURE 5: PERFECTLY PLASTIC AND ELASTIC RESPONSE; WITH (W.R.) AND WITHOUT (N.R.) RESIDUAL STRESSES

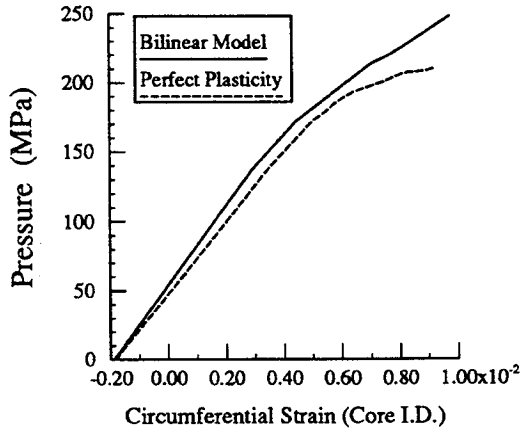

FIGURE 6: COMPARISON OF BILINEAR AND PERFECTLY PLASTIC RESPONSE

two, to the predicted bilinear response at the OD. This comparison is shown in Fig. 8. Clearly, the comparison is quite good. In addition, in Fig. 8, the inner diameter (ID) response curves for the case of bilinear hardening and perfectly plastic are shown to illustrate the difference between the two assumptions. The better agreement with experimental results, in the bilinear case, is believed to be attributed to the more accurate material characterization, as discussed in the previous constitutive model section. Also, it is comforting to note that the experimental data, for ring one, is bounded by the ID and OD bilinear response. Finally, note that ring one had a burst pressure of 190 MPa whereas that of ring two was 155 MPa. The lower burst pressure of ring two was attributed to manufacturing problems.

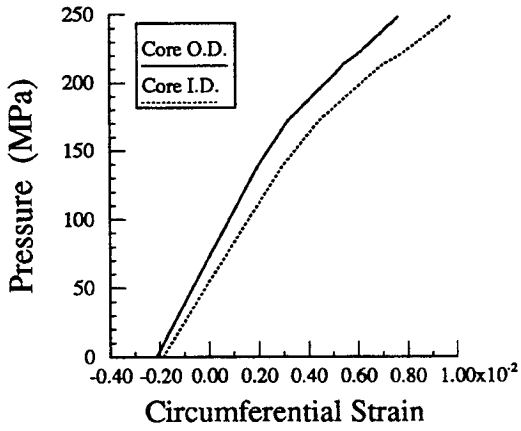

FIGURE 7: RESPONSE AT CORE ID AND CORE OD

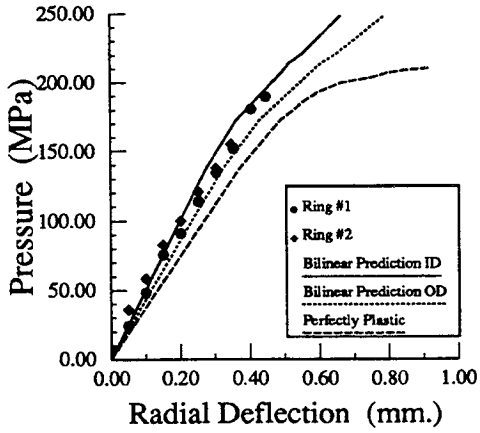

FIGURE 8: COMPARISON OF EXPERIMENTAL AND COMPUTED MECHANICAL RESPONSE

DAMAGE ANALYSIS (FATIGUE LIFE)

Two classes of fatigue life assessments have been performed. The first, and simplest, is a decoupled deformation and damage analysis, that is, one in which no structural stress redistribution (caused by the evolution of damage) is incorporated; thus providing an upper and lower bound on the life of the ring. The second is a coupled deformation and damage analysis and involves the additional complexity of incorporating structural stress redistribution through the degrading of appropriate material properties. Both life assessments are accomplished by employing a recently developed transversely isotropic continuum damage mechanics (CDM) model (see Arnold and Kruch (1991 and 1992)), applicable to unidirectional metallic composites and the previous three dimensional, elastic-plastic, finite element deformation analysis.

The multiaxial, isothermal, fatigue model is phenomenological, stress based, and assumes a single scalar internal damage variable, whose evolution is anisotropic and is associated with the initiation and propagation of transgranular defects. The development of this fatigue damage evolutionary law (model) is founded on the definition of an initially transversely isotropic fatigue limit surface, static fracture surface and normalized stress amplitude function. The anisotropy of the model is defined through physically meaningful invariants reflecting the local stress and material orientation. Finally, the concept of effective stress and remaining life are utilized to measure and interpret damage.

The deformation and damage procedure utilized in this study may be divided into the following 5 steps:

1) Perform a 3-D elastic-plastic FEM deformation analysis in which the ring is subjected to one complete load cycle. For the complete cycle, record the average stress state at different load levels (stress history) for each element in the "representitive strip" of the ring cross-section.
2) For each element and its given stress history, determine the maximum and minimum stress states.
3) The maximum and minimum stress states and the current amount of damage were then used as input for the fatigue damage model. For the present application, the fatigue damage model was implemented using MATHCAD and used in a post-processing life analysis. The input required for the model in MATHCAD was the above mentioned maximum and minimum stress states and the current damage, as well as the material properties. The resulting output is the number of cycles to failure. In addition, for a given increment in damage, i.e. $\Delta D = 0.20$, the corresponding increment in cycles, ΔN is calculated.
4) For the updated measure of damage, D, the associated elastic moduli and yield stress of each element is degraded, i.e., $E^* = E(1-D)$ $G^* = G(1-D)$ $\sigma_y^* = \sigma_y(1-D)$
5) The material constants in the MARC input data are updated/ modified to reflect the current state of damage. Next, step 1 is re-run thus giving the new stress distribution simulating that which would have occurred after an additional ΔN cycles has elapsed.

Steps 2 through 5 are then repeated until the ring has failed (burst). A second approach is also under development at this time, in which the fatigue damage model has been directly linked with

the MARC finite element analysis program through the use of available "user" subroutines provided in MARC. Thus, in this method, no "post-processing" after each load cycle, outside of the finite element analysis, is required. The entire fatigue life analysis may be performed in a single finite element anaylsis run. Additional details of this approach will be presented in forthcoming publications.

Note that when conducting a decoupled deformation and damage analysis stress redistribution is not accounted for steps 1 through 4 are performed only once. That is, the number of cycles to failure of the ring is based upon the initial damage free cyclic stress history. Also note in step 3, the number of cycles, N , that one can take in between deformation analyses was determined by somewhat of a trial and error procedure. It was found that if the amount of material damage, D, was limited to approximately 20% per analysis run, then the amount of stress redistribution incurred within ΔN cycles was reasonable and did not adversely affect the damage accumulation within any given element. Consequently, the increment in damage, in any given element was not allowed to exceed 20%. With this constraint the maximum number of cycles within a given increment was determined (using the element with the current shortest remaining life) and used as the "controlling" ΔN. This ΔN was than applied to all other elements for their damage calculations. The damage associated with each element was than updated as indicated in step 3.

In connection with the deformation analysis, which was conducted to predict the stress-strain distribution that was input to the damage analysis, the assumption of elastic perfectly plastic matrix cladding and elastic bilinear hardening composite core was made. Also, no residual stresses of any kind are accounted for in the associated deformation/damage analysis. For example, no thermal mismatch between either the matrix cladding and composite core (macro mismatch) or the fiber and matrix (micro mismatch) is accounted for, or any residual stress due to incurred plastic deformation from one cycle analysis to another (i.e., each cycle analysis was consider to be independent). Finally, the cusp that resulted from fabrication and discovered using NDE was not included in the deformation analysis.

With respect to the damage model, the damage variable is taken to be a scalar (damage is assumed equivalent in all directions, isotropic) with an evolution that is anisotropic (dependent upon loading direction relative to fiber direction). The concept of effective stress was used in order to allow integration, through the degradation of the elastic and plastic properties, of the damage measure (D) into the deformation analysis. Fiber breakage (D = 1) was assumed to occur whenever the total strain within a given composite element reached 0.8%. This assumption was based on experimental evidence with uniaxial tensile specimens. Lastly, due to the limited data available on the SiC/Ti-15-3 system at 800°F, creep damage and mean stress effects were neglected.

DAMAGE CHARACTERIZATION

The required exploration and characterization experiments for the damage model of are completely described by Arnold and Kruch (1991). Here, because of insufficient data, the shear ratios, η_u, η_{fl}, and η_m were all assumed to be 1.0 (i.e., isotropic in shear) and the longitudinal S-N response (see Fig. 9) was used to obtain the constants; a, β, M_L, σ_{uL} , and σ_{flL}. Then while these constants were held fixed, the three transverse data points were fit to obtain the "strengths" of anisotropy, ω_u, ω_{fl}, and ω_m. Figure 10 shows both the correlations (lines) and the experimental data (symbols) for a 35 fiber percent, longitudinal and transverse SiC/Ti 15-3 system and the Ti-15-3 matrix material at 800°F. Table 3 lists the specific individual material parameters used. Finally, the solid square symbol associated with the transverse (90°) response was not used in the correlation data set for the composite response and therefore represents a check on the predictive capability of the present model at the coupon level. The accuracy is within a factor of 2.

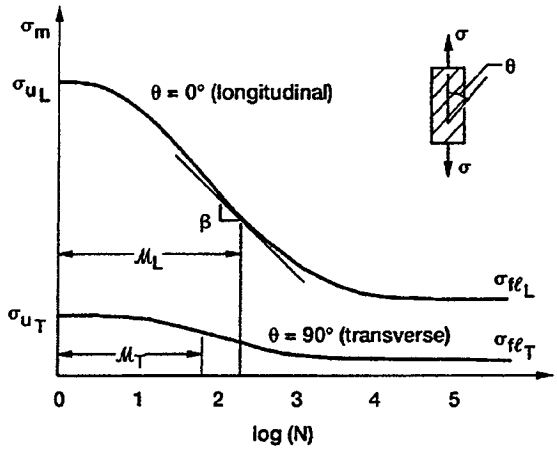

FIGURE 9: S-N CURVES FOR A UNIDIRECTIONAL COMPOSITE

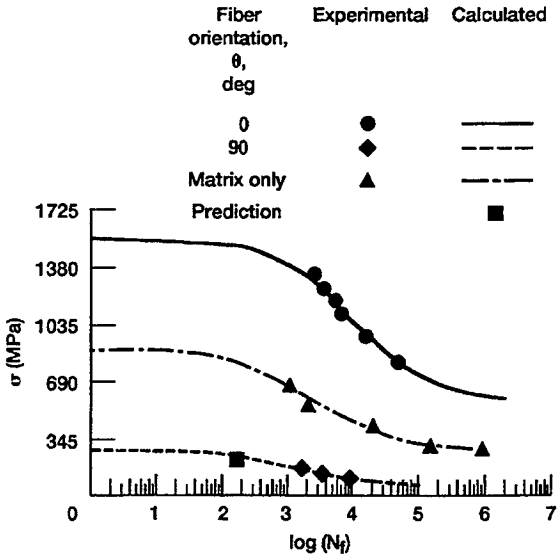

FIGURE 10: CORRELATION OF CDM MODEL AND SIC/TI 15-3 DATA

Table 3: MATERIAL PARAMATERS FOR CDM ANALYSIS

SiC/Ti 15-3 Composite Material

$\sigma_{uL} = 1551.$	$\omega_u = 5.5$
$\sigma_{flL} = 286.$	$\omega_{fl} = 12.482$
$\beta = 1.842$	$\omega_m = 11.8$
$a = 0.065$	$\eta_u = \eta_{fl} = \eta_m = 1.0$
$M = 22371.$	

Matrix Material (Ti-15-3) - Isotropic Simplification

$\sigma_{uL} = 882.$	$\omega_u = 1.0$
$\sigma_{flL} = 140.$	$\omega_{fl} = 1.0$
$\beta = 2.27$	$\omega_m = 1.0$
$a = 0.2302$	$\eta_u = \eta_{fl} = \eta_m = 1.0$
$M = 6205.$	

DAMAGE RESULTS

Given the calculated burst pressure (or limit pressure, P_L) of 221 MPa, four normalized pressure ratios were examined, i.e., P/P_L = 0.35, 0.56, 0.78 and 0.84. The pressure ratio versus cycles to failure results of the decoupled deformation and damage solution, are shown in Fig. 11. In Fig. 11, only the results for the four elements comprising the composite core, in the representative section shown in Fig. 2, are given. As one might expect failure begins at the inner radius and proceeds outward. As a result, failure of the inner element provides one with a lower bound on life, whereas the outer element gives an upper bound on the life of the ring. This type of analysis would be similar to a traditional fatigue initiation analysis.

Figure 12 illustrates the results obtained by performing a coupled deformation and damage analysis, that is one in which redistribution of stress due to damage evolution is accounted for. This type of analysis differs from the typical fatigue analysis since both initiation and propagation of fatigue cracks are incorporated into the damage model. Here each data point represents failure of the ring and not just failure of a given finite element, as in Fig. 11. It is interesting to note that only for pressure levels very near the limit load does the decoupled and coupled analysis compare, thus indicating that at high load levels ring failure is dominated by initiation of inner radius failure within the composite core. The corresponding evolution of damage, throughout the life of the ring is shown in Fig. 13, for the case of $P/P_L = 0.56$ or P = 124 MPa. Figure 13, illustrates clearly the damage state at various percentages of life (N/N_f) over the entire representative strip. Note that inner core radius damage initiates at 35% of the ring's life and that propagation of this damage consumes 65% of the life. Clearly, once failure of the inner core element occurs, the rate of damage progression accelerates dramatically, for this particular load level. A number of significant advantages in utilizing the present continuum damage model over other traditional fatigue models is indicated by comparing Figs. 11 and 12. These are, i) stress redistribution (due to damage evolution) and its impact on life be easily accounted for, ii) damage accumulation can easily be tracked, and iii) a single life value can be obtained without resorting to multiple life assessment analyses, e.g. fatigue initiation failure coupled with a fracture mechanics propagation analysis.

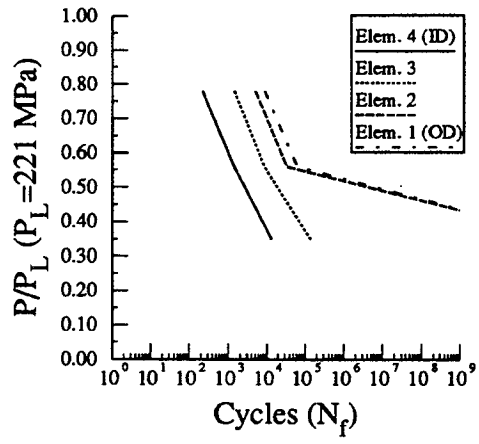

FIGURE 11: DECOUPLED LIFE PREDICTION

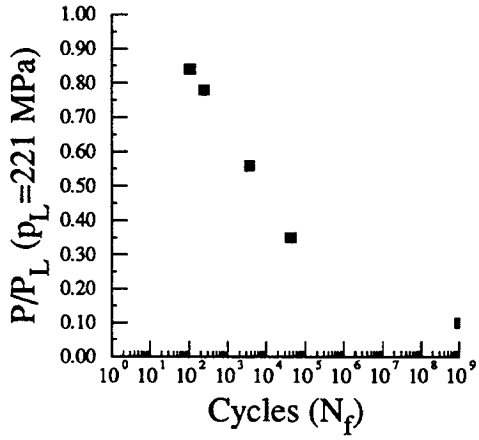

FIGURE 12: COUPLED LIFE PREDICTION

Unfortunately, no experimental fatigue test results are available for comparison to the predicted design life curves, because of premature tensile failure of the remaining MMC rings in this phase of the program due to fabrication problems. Thus no definitive statements can be made regarding the predictive capability of the recently proposed unidirectional continuum damage fatigue model at this time. It is hoped that in the near future additional rings will be fabricated and tested so as to assess the accuracy of the pro-

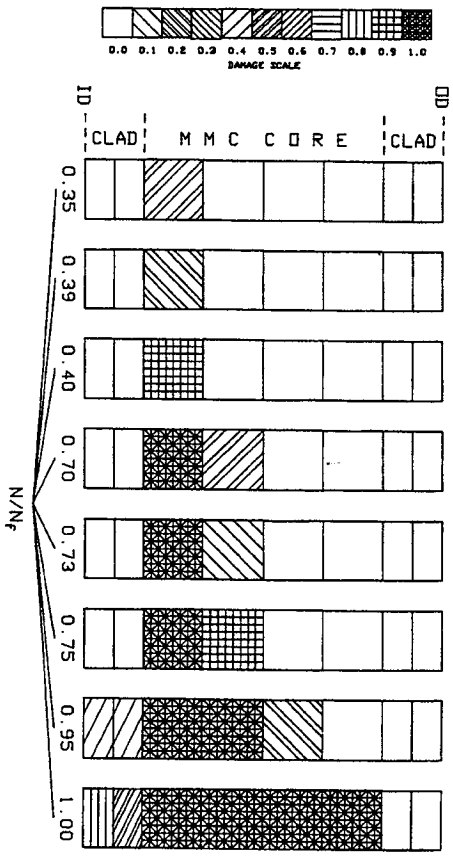

FIGURE 13: DAMAGE EVOLUTION IN REPRESENTITIVE STRIP

posed model at the component level. However, the accuracy at the coupon level appears to be reasonably good as indicated in the previous section.

SUMMARY OF RESULTS

A computational methodology has been developed to predict the fatigue life of typical aerospace components. Here, the specific example was a circumferentially reinforced SiC/Ti-15-3 compressor ring designed for applications at 800°F. The analysis encompassed both a static burst pressure prediction and a decoupled and coupled deformation and damage life assessment of the cladded ring. A three dimensional stress analysis was performed using MARC, a nonlinear finite element code, wherein both the matrix cladding and the composite core were assumed to be behave elastic-plastic. The composite core behavior was represented using Hill's anisotropic continuum based plasticity model with bilinear hardening. Similarly, the matrix cladding was represented by an isotropic perfectly plastic model.

The life assessment was conducted using the finite element stress analysis results, in conjunction with a recently developed multiaxial, isothermal, continuum damage mechanics model for the fatigue of unidirectional metal matrix composites. This model is phenomenological, stress based, and assumes a single scalar internal damage variable, the evolution of which is anisotropic. The accumulation of damage is included in the stress analysis by employing the concept of effective stress. In the current application, however, the damage model is computationally decoupled from the finite element solution. The specific methodology for this computationally- decoupled fatigue damage simulation was outlined and fatigue life predictions were given in terms of design life curves (pressure ratio versus cycles to failure). Finally, a graphical depiction of the damage evolution within a matrix cladded MMC ring was presented.

In general the following conclusions can be made:

1) It was shown that residual stresses do not affect the resulting limit load but do affect the load level corresponding to first yielding.
2) It was shown that the structural load --- displacement (i.e., internal pressure versus radial deflection) response can be obtained reasonably accurately given only coupon data.
3) No definitive conclusion regarding failure, static or fatigue, can be made at this time, because of limited confidence in the fabrication quality of the MMC rings tested.

Work is continuing in the area of fully automating the discussed life assessment methodology by imbedding the fatigue life calculations within the finite element solution scheme/algorithm, thereby, "computationally coupling" the deformation and damage (life) analysis. In addition, fatigue life predictions (simulations) will require the incorporation of so-called "cyclic jump techniques" in the solution scheme. Also, damage analysis using the finite element method results in additional numerical difficulties such as mesh dependent damage propagation, and localization phenomenon. Topics such as these will be addressed in the future.

REFERENCES

Arnold, S.M. and Kruch, S., *Differential Continuum Damage-Mechanics Models for Creep and Fatigue of Unidirectional Metal Matrix Composites*, NASA TM 105213, 1991.

Arnold, S.M. and Kruch, S., *A Differential CDM Model for Fatigue of Unidirectional Metal Matrix Composites, Damage Mechanics in Composites*, D.H. Allen and D. C., Lagoudas, Eds., AMD-Vol. 150, AD-Vol. 32, pp. 213-232, 1992.

Baaklini, G.Y., Percival, L., Yancey, R.N., and Kautz, H.E., *NDE of Titanium MMC Rings for Gas Turbine Engines*, ASME, 10th Biennial Conf. on Reliability, Stress Analysis and Failure Prevention, Albuquerque, New Mexico, Sept. 1993.

Gravett, P.W., *Material Database for P&W/NASA LeRC MMC Life System Development Cooperative Program*, internal communications, Pratt & Whitney, Dec, 1990.

Hill, R., *The Mathematical Theory of Plasticity*, Oxford University Press, 1983.

Lerch, B., private communications, Fatigue and FractureBranch, Structures Division, NASA LeRC.

Robinson, D.N. and Pastor, M.S., *Limit Pressure Of A Circumferentially Reinforced SiC/Ti Ring*, Composite Engineering, Vol. 2, No. 4, pp. 229-238, 1992.